

Research Article

Hyperspherical Manifold for EEG Signals of Epileptic Seizures

Tahir Ahmad and Vinod Ramachandran

*Ibnu Sina Institute for Fundamental Science Studies, Universiti Teknologi Malaysia,
81310 Skudai, Johor, Malaysia*

Correspondence should be addressed to Tahir Ahmad, tahir@utm.my

Received 3 February 2012; Revised 11 April 2012; Accepted 21 April 2012

Academic Editor: E. S. Van Vleck

Copyright © 2012 T. Ahmad and V. Ramachandran. This is an open access article distributed under the Creative Commons Attribution License, which permits unrestricted use, distribution, and reproduction in any medium, provided the original work is properly cited.

The mathematical modelling of EEG signals of epileptic seizures presents a challenge as seizure data is erratic, often with no visible trend. Limitations in existing models indicate a need for a generalized model that can be used to analyze seizures without the need for apriori information, whilst minimizing the loss of signal data due to smoothing. This paper utilizes measure theory to design a discrete probability measure that reformats EEG data without altering its geometric structure. An analysis of EEG data from three patients experiencing epileptic seizures is made using the developed measure, resulting in successful identification of increased potential difference in portions of the brain that correspond to physical symptoms demonstrated by the patients. A mapping then is devised to transport the measure data onto the surface of a high-dimensional manifold, enabling the analysis of seizures using directional statistics and manifold theory. The subset of seizure signals on the manifold is shown to be a topological space, verifying Ahmad's approach to use topological modelling.

1. Introduction

Epilepsy is a chronic disorder of the brain that affects people all over the world. It is characterized by recurrent seizures—physical reactions to sudden, usually brief, excessive electrical discharges in a group of brain cells [1].

Seizures are classified into two major categories, partial seizures and generalized seizures. Partial seizures are those in which the clinical or electroencephalographic evidence suggests that the attacks have a localized onset in the brain [2]. This type involves only a part of the cerebral hemisphere at seizure onset and produces symptoms in corresponding parts of the body or disturbances in some related mental functions [3]. On the contrary, generalized seizures are said to occur if the evidence suggests that the attacks were well spread [4].

The diagnosis and treatment of epilepsy is greatly aided by the use of electroencephalography as a monitoring tool.

Electroencephalography (commonly referred to by its abbreviation EEG) is the measurement of electrical activity produced by the firing of neurons in the brain. It operates by recording the fluctuations in the potential difference of electrodes attached to the scalp of a patient, with these fluctuations indicating the presence of neural activity [5]. In practice, computerized systems such as NicoletOne are used to digitize EEG signals before they are subjected to statistical analysis. It is not uncommon for the interpretation of clinical EEG to involve speculation as to the possible locations of the source(s) inside the brain which are responsible for the observed activity on the scalp [4]. The mathematical analysis of EEG signals aids medical professionals by providing a description of the brain activity being observed, thus increasing the understanding of human brain function.

2. Related Work

To date, numerous methods have been employed in the mathematical modelling of epileptic seizures, each with varying objectives and results.

In 1986, Babloyantz and Destexhe used the time series of EEG data during a seizure to show the presence of deterministic dynamics of a complex nature for seizures [6]. By identifying and comparing the chaotic attractors during (*ictal*) and between (*interictal*) seizures, they argued that an epileptic seizure is a low-dimensional state, which was further clarified by Stam as a “loss of complexity” [7]. This concept was further strengthened by Iasemidis et al. by computing the decrease of the largest Lyapunov exponent during an epileptic seizure [8], a result which was further corroborated in 1990 by Frank’s analysis of the EEG of absence seizures, in which he indicated the existence of an underlying chaotic attractor [9]. However, Theiler’s analysis of the same dataset showed that the supposed chaotic properties can be attributed to a noisy limit cycle [10]. Support for this opposing view can be seen in studies by Schiff et al. [11], Friedrich and Uhl [12], Hernandez et al. [13], Le van Quyen et al. [14], and Feucht et al. [15], which leads to the conclusion that the use of time series modelling is highly dependent on the quality of the EEG signals produced. In practice, a noise filter is applied prior to signal amplification to help remove white noise. However, one inherent problem with EEG recordings of seizures is the crossing of its input and output sets—all recorded signals (gross output) are a combination of seizure activity (net output), exogenous noise, and the current source used to generate a potential difference between two electrodes (net input). Hence, to accurately model a seizure, dynamical noise reduction needs to be applied to isolate the signals generated from seizure activity alone, which in turn results in degradation of the source signal.

Nevertheless, modelling of the EEG signals of epileptic seizures endured, with focus shifting to forecasting brainstorms, reasoning for which is the ability to warn and prepare treatment for an impending seizure. The ultimate goal is to produce a closed system where a patient can be connected to an automated device that predicts the onset of seizures and administers the appropriate medication as necessary, a concept that was first outlined by Peters et al. in 2001 [16]. When it came to forecasting brainstorms, nonlinear models took preference over linear models. Studies conducted by Elger and Lehnertz [17], and Martinerie et al. used intercranial EEG to show that seizures can be anticipated, sometimes up to 5 minutes in advance [18]. In 2001, Le van Quyen demonstrated that seizure prediction can be carried out with surface recordings alone [7], jumpstarting research into noninvasive models for seizure prediction. Consequently, various approaches were employed to model

seizures, including Lyapunov exponents [19] (shown to be inapplicable for low-dimensional deterministic chaotic systems such as epileptic seizures by Lai et al. in 2003 [20]), correlation integrals and dimensions [21] (also shown to be inapplicable for epileptic seizures [22]), phase clustering [8, 23], and entropy measures [24]. Although some of these models were quite successful, they are very specific in nature, only being able to model a very small subset of seizures, a common flaw in nonlinear models. Additionally, Mormann et al. have highlighted that although most of the studies published in the 1990s and around the turn of the millennium yielded rather promising results, more recent evaluations could not reproduce these optimistic findings [25].

It was only after analysis of Martinerie's earlier work that McSharry et al. discovered that linear measures could also be used to model seizures [26]. The acceptability of linear models was solidified with Kugiumtzis and Larsson concluding that nonlinear methods offered no significant advantage over linear models [27]. This result was followed up in 2001 by Jerger, who compared 7 different linear and nonlinear measures and found that both classes of measures produced similar results [28]. This provided strength to existing linear models, such as Baillet and Garnero's Bayesian-based model [29]. Although Bayesian modelling proved successful, its reliance on apriori information yields a low level of accuracy for patients who have a low occurrence of seizures. Furthermore, additional data cannot be generated by inducing seizures, as the Pavlovian effect on seizure provocation is still undetermined [30]; that is, researchers are unable to identify if repeated seizure provocation results in specific brain cells being conditioned to react to stimuli, thus jeopardizing the integrity of the data obtained.

With the introduction of new mathematical tools over the last decade, more complex models were developed. In 2008, Faust et al. successfully applied Burg autoregressive coefficients in the modelling of epileptic seizures, achieving an accuracy of over 90% in detecting seizures [31]. This result was bettered by Sivasankari and Thanushkodi in 2009 using fast independent component analysis coupled with neural networks [32]. These methods, although highly successful, are of high complexity and are notoriously resource-intensive.

In 2000, Ahmad et al. formulated a fuzzy-based topological model to identify the foci of an epileptic seizure [33]. The model, called Fuzzy Topographic Topological Mapping (FTTM), involves inducing a topology on the magnetic field of magnetoencephalographic (MEG) recordings and utilizes fuzzy techniques to estimate the location of the epileptic foci [34]. The epileptic foci here refer to points in the brain from which the seizures are assumed to originate. This method was further refined in 2008 to include EEG input [3]. Apart from estimating the epileptic foci, the FTTM method is able to index key events during the progression of seizures, as demonstrated in Idris's 2010 paper [35]. Despite its successes, the model has drawn some criticism due to the loss of information incurred during the fuzzification/defuzzification process. By using the same set of patient data as Ahmad, this research aims to provide a foundation for the geometric modelling of statistical data of seizures without the use of fuzzy theory.

3. Contributions

The contributions of this paper are as follows.

- (1) A discrete probability measure called the Delia measure is developed. Usage of this measure overcomes the need for apriori information without compromising the structural pattern of the inputted data.

- (2) Digitized raw EEG data is processed using the developed measure. Subsequent analysis shows success in highlighting specific areas of the brain which show a large change in potential difference. In the case of three patients who are known to demonstrate physical symptoms, the model successfully identifies increased potential differences in areas of the brain that correspond to the observed symptoms.
- (3) A mapping from the set of seizure measure values to a unit hypersphere is defined. This results in a manifold for EEG signals of seizures, thus enabling further analysis of seizures using directional statistics and manifold theory.
- (4) The set of EEG signals on the manifold is shown to constitute a topological space, thus verifying Ahmad's use of topological modelling.

4. Preliminaries

In this section, some existing definitions and/or results that will be used in this paper are introduced.

4.1. Probability and Measure

The first part of this paper will be the development of a probability measure, purpose-suited to measuring EEG signals detected during epileptic seizures. The given definitions below are primarily sourced from measure theory, motivation of which is given in Section 5.

Definition 4.1 (σ -algebra). Suppose X is a set and \mathcal{A} is a collection of subsets of X . \mathcal{A} is called a σ -algebra of subsets of X provided it contains the set X and is closed under taking complements (with respect to X), countable unions, and countable intersections [36].

Definition 4.2 (set function). A set function is a function ν whose domain of definition is a nonempty class \mathcal{E} of sets [37].

Definition 4.3 (measure). A measure is defined as a set function μ whose domain of definition is a ring \mathcal{R} , such that

- (1) μ is additive;
- (2) μ is positive;
- (3) $\mu(\emptyset) = 0$;
- (4) if E_n is an increasing sequence in \mathcal{R} whose union E is also in \mathcal{R} , then $\mu(E) = \text{lub}[\mu(E_n)]$ [37].

Definition 4.4 (measurable space). A measurable space is a pair (X, \mathcal{D}) , where \mathcal{D} is a σ -ring of subsets of X . Elements of \mathcal{D} are said to be measurable [37].

Definition 4.5 (probability space). A probability space is a measurable space with total measure 1, that is if X is a probability space, and μ is the measure defined on X , then $\mu(X) = 1$ [38].

Definition 4.6 (discrete random variable). A discrete random variable is a numerical quantity that, in some experiment that involves some degree of randomness, takes one value from some discrete set of possible values [39].

Definition 4.7 (probability mass function). Let X be a discrete random variable. A probability mass function for X is a function $p(x)$ which assigns a probability to each value of the random variable such that

- (1) $p(x) \geq 0$ for all x , and
- (2) $\sum p(x) = 1$ [40].

Definition 4.8 (Kolmogorov-Smirnov test). The Kolmogorov-Smirnov test is designed to test $H_0 : F(x) = G(x)$, for all x versus $H_0 : F(x) \neq G(x)$ for at least one x , where $F(x)$ and $G(x)$ are distributions associated with two independent groups [41].

Definition 4.9 (von Mises-Fisher distribution). A d -dimensional random unit vector is said to have a d -variate von Mises-Fisher distribution if its probability density function is given by

$$f(x | \mu, \kappa) = c_d(\kappa) e^{\kappa \mu^T x}, \quad (4.1)$$

where $\|\mu\| = 1$, $\kappa \geq 0$, and $d \geq 2$. The normalizing constant $c_d(\kappa)$ is given by

$$c_d(\kappa) = \frac{\kappa^{(d/2)-1}}{(2\pi)^{d/2} I_{(d/2)-1}(\kappa)}, \quad (4.2)$$

where I_r represents the modified Bessel function of the first kind with order r . μ is known as the mean vector, and κ is called the concentration parameter [42].

4.2. Topology and Manifolds

This section covers some basics on topology and manifold theory that will be used to map the EEG signals to a manifold.

Definition 4.10 (Euclidean n -space). Euclidean n -space, E^n , is the set of all possible ordered n -tuples of real numbers, that is, $E^n = \{(x_1, x_2, \dots, x_n) | x_i \in \mathbb{R}\}$ [43].

Definition 4.11 (hypersphere). A hypersphere or n -sphere is given as $S^{n-1} = \{x \in \mathbb{R}^n | \|x\| = r\}$, where r denotes the radius of the hypersphere. A hypersphere with radius 1 is called a unit hypersphere [44].

Definition 4.12 (manifold). Let S be a set. If there exists a set of coordinate systems \mathcal{A} for S which satisfies the following 2 conditions.

- (1) Each element ϕ of \mathcal{A} is a one-to-one mapping from S to some open subset of \mathbb{R}^n ;
- (2) for all $\phi \in \mathcal{A}$, given any one-to-one mapping ψ from S to \mathbb{R}^n , $\psi \in \mathcal{A} \Leftrightarrow \psi \circ \phi^{-1}$ is a C^∞ diffeomorphism.

Then (S, \mathcal{A}) is called a manifold [45].

Theorem 4.13 (hyperspheres as manifolds). *The hypersphere S^{n-1} is a manifold [46].*

The proof of Theorem 4.13 is trivial, and is hereby skipped. For the complete proof, refer to Lee's treatment of topological manifolds [46].

Definition 4.14 (topological space). Let X be a nonempty set. A class τ of subsets of X is a topology on X if and only if τ satisfies the following axioms:

- (1) X and \emptyset belong to τ ;
- (2) The union of any number of sets in τ belongs to τ ;
- (3) The intersection of any two sets in τ belongs to τ .

The members of τ are called τ -open sets, or simply open sets, and X together with τ , that is the pair (X, τ) is called a topological space [47].

Definition 4.15 (topological subspace). Let X be a topological space, and let $S \subseteq X$ be any subset. The subset topology τ_S on S is defined by

$$\tau_S = \{U \subseteq S \mid U = S \cap V \text{ for some open subset } V \subseteq X\}. \quad (4.3)$$

The pair (S, τ_S) is called a topological subspace of X [46].

4.3. L_p -Normalization

L_p -normalization is the process of scaling a given vector in p -dimensional space so that its L_p norm meets a specific value. It is commonly used in data mining applications such as text categorization and gene expression analysis, where the data possesses a high dimension and is inherently directional in nature [42]. The L_p norm of a vector is defined as follows.

Definition 4.16 (L_p -norm). For a vector x , the L_p -norm is given by

$$\|x\| = \left(\sum_{i=1}^{\infty} |x_i|^p \right)^{1/p}. \quad (4.4)$$

A special case of the L_p norm is when $p = 2$, where the norm is called the Hilbert norm [48].

There is no unique method of carrying out the normalization, as any suitable transformation can be used, provided the resulting L_p norm meets its desired value. Common transformations include the use of trigonometric operators, and division by a common factor.

5. Measure Construction

During an epileptic seizure, EEG electrodes are attached to the patient's scalp and the resulting potential differences are recorded. To standardize the locations from which the potential differences were recorded, a system of electrode placement was introduced, called the International 10–20 System [49].

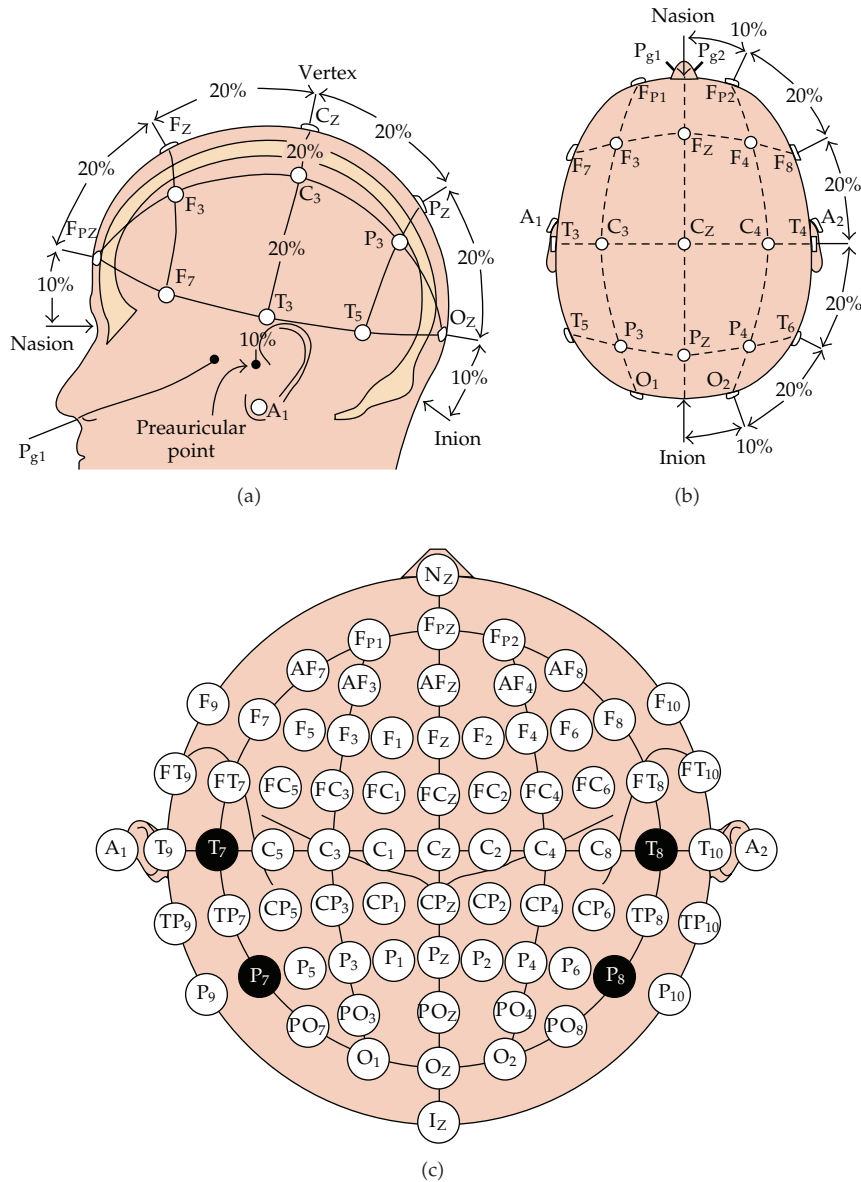


Figure 1: Standard electrode positioning as per the International 10–20 system [49].

The seizure data used in this research is that utilized by Ahmad in his work, where 25 (21 active and 4 reference) electrodes are attached to a patient’s head in accordance with the International 10–20 System. The standard electrode positioning for this system is illustrated in Figure 1. When a seizure occurs, the data is recorded and trimmed to correspond to the period of ictal. To mathematically identify the EEG signals observed by their respective electrodes, the set of electrodes used in this research is introduced as the *electrode set*.

Definition 5.1 (electrode set). The standard set of all monitored EEG electrodes during an epileptic seizure is called the electrode set, E , and is given by

$$E = \{e_1, e_2, \dots, e_n\}, \quad (5.1)$$

where e_i represents an EEG electrode that is being monitored during an epileptic seizure.

In this study, the electrode set utilized is

$$E = \{F_{P1}, F_{P2}, F_3, F_4, C_3, C_4, P_3, P_4, O_1, O_2, F_7, F_8, \\ T_3, T_4, T_5, T_6, A_1, A_2, F_Z, C_Z, P_Z, T_7, T_8, P_7, P_8\}. \quad (5.2)$$

Elements of the electrode set serve as indices to indicate the electrode at which a particular set of electrical potentials is detected.

Definition 5.2 (reference subset). The subset of the electrode set that contains only reference electrodes is called the reference subset, R , and is given by:

$$R = \{e \in E \mid e \text{ is a reference electrode}\}. \quad (5.3)$$

In this study, the reference subset utilized is:

$$R = \{T_7, T_8, P_7, P_8\}. \quad (5.4)$$

Definition 5.3 (electrode potential set). In any given patient, the set of all potential differences detected during a seizure at time t is given by

$$V_t = \{v_e \mid v_e \in \mathbb{R}, e \in E \setminus R\}, \quad (5.5)$$

where v_e is the potential difference detected at electrode e at time t in relation to its closest reference electrode. We call V_t the electrode potential set at time t .

Prior to developing a custom measure, the data was tested for conformity to existing distributions. The data was analyzed twice, first using the electrodes as the independent variable, and again using one-second time frames as the independent variable. Taking electrodes as the independent variable allow a seizure to be viewed as a breakdown of potential differences detected across monitored electrodes at any fixed one-second time frame. Alternatively, taking time frames as the independent variable results in a view of the progression of a seizure in terms of the potential differences detected at each electrode over a given period of time. Visual inspection using Q - Q plots show that although some electrodes display characteristics that are close to that of normal and log-normal distributions, the same does not hold for all electrodes. As for the one-second time frame case, similar behavior is observable, as can be seen from Figures 2 and 3. Furthermore, Kolmogorov-Smirnov (K-S) testing at a tolerance level of 0.5 reveals that the data does not entirely conform to that of normal, uniform, nor exponential distributions.

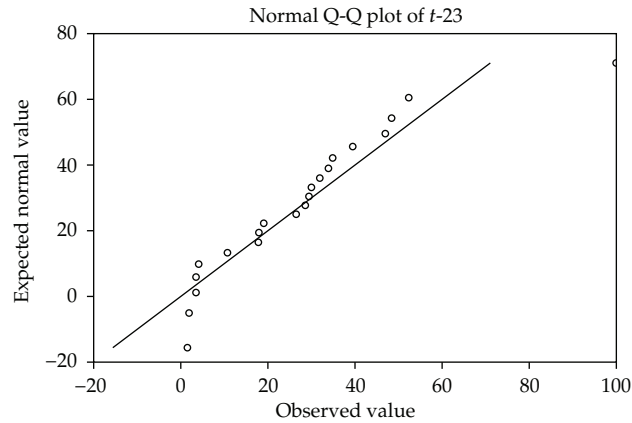


Figure 2: Q-Q of potential differences detected at time $t = 23$ s during a seizure. The data collected at this time frame conforms to that of a power law distribution.

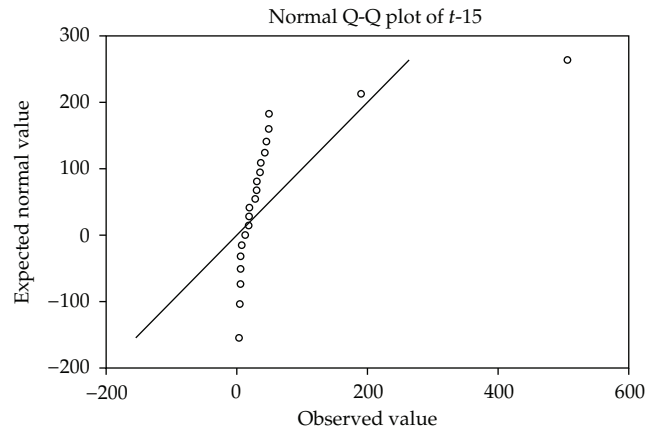


Figure 3: Q-Q of potential differences detected at time $t = 15$ s during the same seizure. Note that the data no longer displays normal tendencies.

To compare the progression of one seizure to another, a general probability distribution that applies to all recorded events during the seizure is required. A generalized nonlinear model is most suited to the task, but limited understanding on the factors that influence a seizure results in a poorly designed model. Given that some electrodes display normal tendencies (including the power law distribution), the authors conjecture that the von Mises-Fisher (vMF) distribution is a natural candidate to represent an epileptic seizure. As mentioned in Section 2, Babloyantz and Destexhe describe a seizure as a low-dimensional state, which Stam calls a “loss of complexity.” This loss of complexity can be explained as a loss of structural information in the seizure data, resulting in a vMF distribution to appear somewhat normal in lower dimensions. Furthermore, the use of a hypersphere to describe a seizure gives the data a fixed structure to lie on, thus confining seizure data to a specific surface. This upscale is possible as a point in a lower dimension is topologically equivalent to its counterpart in a higher dimension.

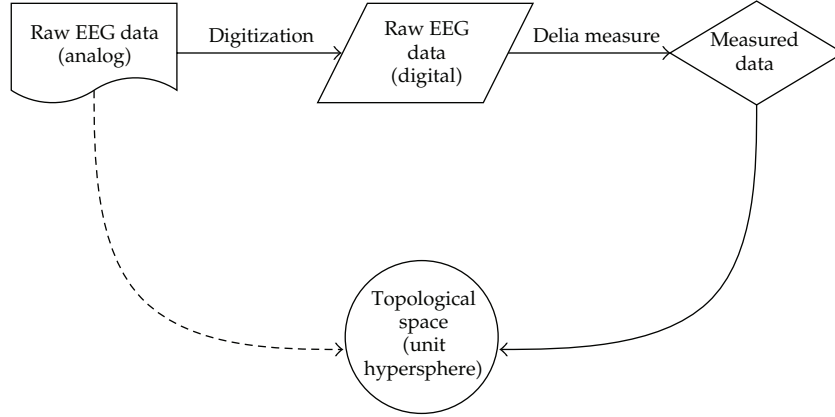


Figure 4: Pathway to mapping EEG signals to a manifold.

As mentioned in Section 2, Bayesian modelling is highly dependent on apriori information. As a workaround to assigning probability values based on data derived from prior seizures, a simple measure is designed based on the deviation from the average signal strength being read by the EEG apparatus during a seizure. This allows seizures to be modelled using instantaneous data, thus eliminating the need for multiple measurements. The measure serves as a foothold for transferring the seizure data to a hypersphere so the vMF distribution can be applied. A simplified process flow diagram of the route taken by the authors is given in Figure 4.

To define a probability measure on V_t , a σ -algebra is constructed on the set. Lemma 5.4 illustrates that the choice of σ -algebra to be defined is simple, namely, the power set of V_t .

Lemma 5.4 (σ -algebra of V_t). *The power set of V_t defines a σ -algebra on the electrode potential set.*

Proof. The power set of an electrode potential set $V_t = \{v_{F_{P1}}, v_{F_{P2}}, \dots, v_{F_{PZ}}\}$ is given by

$$P(V_t) = \{\emptyset, \{v_{F_{P1}}, \dots, v_{F_{PZ}}\}, V_t\}. \quad (5.6)$$

Observe that

- (1) $\emptyset \in P(V_t)$,
- (2) $V_t \in P(V_t)$ since $V_t = \{v_{F_{P1}}, v_{F_{P2}}, \dots, v_{F_{PZ}}\} \in P(V_t)$,
- (3) $\emptyset^c \in P(V_t)$ since $\emptyset^c = V_t \setminus \emptyset = V_t \in P(V_t)$,
- (4) $V_t^c \in P(V_t)$ since $V_t^c = V_t \setminus V_t = \emptyset \in P(V_t)$,
- (5) for any $A, B \in P(V_t)$, $A \cup B \in P(V_t)$ since all elements of $P(V_t)$ are subsets (proper or improper) of V_t , and the union of any number of these subsets cannot exceed V_t ,
- (6) for any non-empty $A, B \in P(V_t)$, $A^c, B^c \in P(V_t)$ since $A^c = V_t \setminus A$ and $B^c = V_t \setminus B$ are proper subsets of V_t , and thus must belong to the power set of V_t ,
- (7) for any $A, B \in P(V_t)$, $A \cap B = (A^c \cup B^c)^c$ by De Morgan's law. Note that A^c and B^c are both in $P(V_t)$ by (6). Applying (5), we have that $A^c \cup B^c \in P(V_t)$. Applying (6), we see that $A \cap B = (A^c \cup B^c)^c \in P(V_t)$.

Thus, $P(V_t)$ defines a σ -algebra on V_t as per Definition 4.1. □

Table 1: Result of K-S testing against a normal distribution for a 10-second seizure.

	$t = 1$	$t = 2$	$t = 3$	$t = 4$	$t = 5$
Mean	97.40	77.92	75.21	50.70	81.70
Std. Dev	112.47	72.14	61.77	50.16	58.18
K-S Z	1.35	1.03	1.03	1.08	.64
Asymp. Sig. (2-tailed)	.05	.24	.24	.19	.80
	$t = 6$	$t = 7$	$t = 8$	$t = 9$	$t = 10$
Mean	116.53	137.22	144.79	129.05	97.92
Std. Dev	104.45	125.66	106.72	93.47	101.03
K-S Z	.68	1.13	.89	.86	1.18
Asymp. Sig. (2-tailed)	.75	.16	.41	.46	.12

Lemma 5.4 leads to the following theorem.

Theorem 5.5 (measurability of elements of $P(V_t)$). $(V_t, P(V_t))$ is a measurable space, and the elements of $P(V_t)$ are measurable.

Proof. By Lemma 5.4, $P(V_t)$ is a σ -algebra on V_t , that is, it is a σ -ring that contains V_t . Thus $(V_t, P(V_t))$ is a measurable space by Definition 4.4, and the measurability of elements of $P(V_t)$ is implied. \square

For the purpose of modelling EEG signals of epileptic seizures, inspiration for the measure is drawn from the standard score, which is commonly used in normalizing data sets. As with most measures, the intended measure will have parameters, that is certain variables that characterize the behavior of the measure. These parameters are the *emulated baseline* and *jitter*, and are defined as follows.

Definition 5.6 (emulated baseline). The emulated baseline, β_t , is the average magnitude of electrical potentials detected across all monitored electrodes at a given time t in a seizure and is given by

$$\beta_t = \frac{\sum_{i=1}^n |v_i|}{n} \quad \text{for } v_i \in V_t. \quad (5.7)$$

Definition 5.7 (jitter). The jitter, δ_t , is the total difference in magnitude of detected electrical potentials and the emulated baseline at a given time t in a seizure and is given by

$$\delta_t = \sum_{i=1}^n ||v_i| - \beta_t| \quad \text{for } v_i \in V_t. \quad (5.8)$$

The emulated baseline and jitter represent the mean and standard deviation of the data set, respectively, with the change in terminology due to the nature of the data being recorded, that is, electrical signals. A sample of the computed emulated baseline and jitter values for a 10-second seizure is given in Table 1. The resulting measure, the *Delia EEG measure*, is formally introduced below.

Definition 5.8 (Delia EEG measure). The Delia EEG measure, μ , is a measure defined on the power set of an electrode potential set, and is given by the set function:

$$\mu : P(V_i) \longrightarrow \mathbb{R}_e \quad \text{such that } \mu(A) = \begin{cases} 0 & \text{if } n(A) = 0, \\ \sum_{i=1}^n \left| \frac{|v_i| - \beta}{\delta} \right| & \text{otherwise,} \end{cases} \quad (5.9)$$

where $v_i \in A$, $A \in P(V_i)$, $n(A)$ is the number of elements in the set A , and \mathbb{R}_e is the set of extended reals.

The following lemma verifies that the set function described in Definition 5.8 satisfies the requirements to be a measure.

Lemma 5.9 (measure property of the Delia set function). *When defined on the power set of an electrode potential set, the set function μ is a measure.*

Proof. Note that elements of V_i are mutually exclusive, that is, $A \cap B = \emptyset$ holds for any $A, B \in P(V_i)$ since no two potential differences can be recorded at one electrode at the same time.

(1) Pick any $A, B \in P(V_i)$ such that $A \cap B = \emptyset$ and consider the following cases:

(a) Case I. Let $A = B = \emptyset$

$$\begin{aligned} \mu(A \cup B) &= \mu(\emptyset \cup \emptyset) \quad \text{since } A = B = \emptyset \\ &= \mu(\emptyset) \\ &= 0 \quad \text{by definition of } \mu \\ &= 0 + 0 \\ &= \mu(\emptyset) + \mu(\emptyset) \quad \text{by definition of } \mu \\ &= \mu(A) + \mu(B) \quad \text{since } A = B = \emptyset. \end{aligned} \quad (5.10)$$

(b) Case II. Let $A \neq \emptyset$, $B = \emptyset$

$$\begin{aligned} \mu(A \cup B) &= \mu(A \cup \emptyset) \quad \text{since } B = \emptyset \\ &= \mu(A) \\ &= \mu(A) + 0 \\ &= \mu(A) + \mu(\emptyset) \quad \text{by definition of } \mu \\ &= \mu(A) + \mu(B) \quad \text{since } B = \emptyset \end{aligned} \quad (5.11)$$

If $A = \emptyset$, $B \neq \emptyset$, merely swapping the sets A and B .

(c) Case III. Let $A \neq \emptyset$, $B \neq \emptyset$

$$\begin{aligned}\mu(A \cup B) &= \sum_{i=1}^n \left| \frac{|v_i| - \beta}{\delta} \right| \quad \text{where } v_i \in A \cup B \\ &= \left| \frac{|v_1| - \beta}{\delta} \right| + \left| \frac{|v_2| - \beta}{\delta} \right| + \dots \\ &\quad + \left| \frac{|v_j| - \beta}{\delta} \right| + \left| \frac{|v_{j+1}| - \beta}{\delta} \right| + \dots \\ &\quad + \left| \frac{|v_n| - \beta}{\delta} \right|\end{aligned}\tag{5.12}$$

rearrange and reindex the above so that

$$v_i \in \begin{cases} A & \text{for } i = 1, 2, \dots, j \\ B & \text{for } i = j + 1, j + 2, \dots, n \end{cases}\tag{5.13}$$

then

$$\begin{aligned}\mu(A \cup B) &= \sum_{i=1}^j \left| \frac{|v_i| - \beta}{\delta} \right| + \sum_{i=j+1}^n \left| \frac{|v_i| - \beta}{\delta} \right| \\ &= \mu(A) + \mu(B).\end{aligned}\tag{5.14}$$

Hence μ is additive for mutually exclusive sets.

(2) Picking any $A \in P(V_t)$,

$$\mu(A) = \begin{cases} 0 & \text{if } n(A) = 0 \\ \sum_{i=1}^n \left| \frac{|v_i| - \beta}{\delta} \right| & \text{otherwise.} \end{cases}\tag{5.15}$$

Thus μ is positive since $|(v_i| - \beta)/\delta| \geq 0$.

(3) $\mu(\emptyset) = 0$ since $n(\emptyset) = 0$ and $\mu(A) = 0$ for any set A such that $n(A) = 0$ (by definition).

(4) Consider a sequence $\{A\}_n$ of increasing sets in $P(V_t)$, that is, $A_1 \subset A_2 \subset \dots \subset A_n$. Observe that A_2 can be rewritten as $A_2 = (A_2 - A_1) \cup A_1$. Thus,

$$\begin{aligned}\mu(A_2) &= \mu[(A_2 - A_1) \cup A_1] \\ &= \mu(A_2 - A_1) + \mu(A_1) \geq \mu(A_1) \quad \text{since } (A_2 - A_1) \cap A_1 = \emptyset.\end{aligned}\tag{5.16}$$

Similarly,

$$\begin{aligned}
 \mu(A_2) &\leq \mu(A_3) \\
 \mu(A_3) &\leq \mu(A_4) \\
 &\vdots \\
 \mu(A_{n-1}) &\leq \mu(A_n).
 \end{aligned} \tag{5.17}$$

Hence, the lub of $\mu(\{A\}_n)$ is $\mu(A_n)$. Denote the union of all sets in $\{A\}_n$ as A . Then,

$$\begin{aligned}
 A &= \bigcup_{i=1}^n A_i \\
 &= A_1 \cup A_2 \cup \dots \cup A_n \\
 &= A_n \quad \text{since } A_1 \subset A_2 \subset \dots \subset A_n.
 \end{aligned} \tag{5.18}$$

Therefore, $\mu(A) = \mu(A_n)$, and, consequently, $\text{lub}[\mu(\{A\}_n)] = \mu(A)$. Thus μ is a measure by Definition 4.3. \square

The following lemma shows that the Delia EEG measure can be used as a probability measure on the electrode potential set.

Lemma 5.10 (measure of V_t). *The total measure of V_t is 1 with respect to μ .*

Proof. The total measure of $V_t = \{v_1, v_2, \dots, v_n\}$ is given by

$$\begin{aligned}
 \mu(V_t) &= \mu(\{v_1, v_2, \dots, v_n\}) \\
 &= \sum_{i=1}^n \left| \frac{|v_i| - \beta}{\delta} \right| \\
 &= \sum_{i=1}^n \frac{||v_i| - \beta|}{|\delta|} \\
 &= \sum_{i=1}^n \frac{||v_i| - \beta|}{\delta} \quad \text{since } \delta \text{ is nonnegative} \\
 &= \frac{1}{\delta} \sum_{i=1}^n ||v_i| - \beta| \quad \text{Since the value of } \delta \text{ is constant } \forall v_i \in V_t \\
 &= \frac{1}{\delta} \cdot \delta \quad \text{since } \delta = \sum_{i=1}^n ||v_i| - \beta| \quad \text{by Definition 5.7} \\
 &= 1
 \end{aligned} \tag{5.19}$$

Thus, V_t has a total measure of 1 with respect to μ . \square

Table 2: Emulated baseline and jitter values for a 10-second seizure (Patient A).

Time (t)	β_t	δ_t
1	98.00806	1586.979
2	78.68421	1036.199
3	76.41594	1040.109
4	51.93148	892.6314
5	78.81386	939.0676
6	120.1871	1672.974
7	143.4501	2120.952
8	150.1537	1754.462
9	132.2427	1533.646
10	99.98561	1576.88

With Lemma 5.10, the following theorem can be proven.

Theorem 5.11 (probability space of EEG signals). (V_t, μ) is a probability space.

Proof. By Theorem 5.5 and Lemma 5.10, V_t is a measurable space with total measure 1 with respect to μ . Thus, by Definition 4.5, V_t is a probability space. \square

The Delia measure μ operates as a probability mass function (PMF), assigning each element $v_i \in P(V_t)$ a probability value $\mu_t(v_i)$. The following section details the application of the measure to data sets of three patients experiencing epileptic seizures.

6. Measure Implementation

The EEG signal data of three patients A, B, and C, suffering from epileptic seizures were modelled using the Delia measure. Emulated baseline and jitter values are first computed from the raw EEG data. Table 2 gives an example of the emulated baseline and jitter values for a 10-second seizure experienced by Patient A.

A plot of μ versus t shows the progression of neural activity at any specific electrode in comparison to the rest. Due to the nature of the measure, ratio of signals in one electrode to another is identical to that of the unprocessed signal, that is, the geometric structure of the signal remains unchanged. μ can be physically interpreted as the rate of seizure activity at any specific electrode relative to all other monitored electrodes. This gives a simplified view of the seizure, with emphasis on electrodes that show the most changes in activity.

As an example, Figure 5 shows that two electrodes display significant changes in measure value throughout the seizure, namely, electrodes F_{P1} and F_{P2} . Core seizure activity takes place in the range of 0.00–0.15, indicating that the majority of the signals detected deviate from the emulated baseline by at most 0.15 units. Both of the electrodes F_{P1} and F_{P2} are situated near the prefrontal cortex, which accounts for the behavioral changes associated with some epileptic patients [50, 51].

Comparatively, the measure data of Patient B (Figure 6) exhibits sharp fluctuations in the potential difference detected at electrode F_8 , which is situated at the premotor cortex of the right hemisphere of the brain, which is the section of the brain that is responsible for sensory guidance of movement and control of proximal and trunk muscles of the body [52].

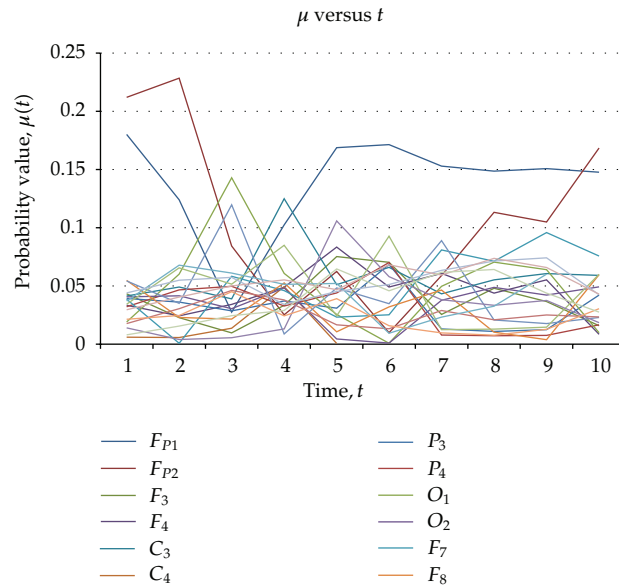


Figure 5: Plot of measure values over time for a 10-second seizure observed in Patient A.

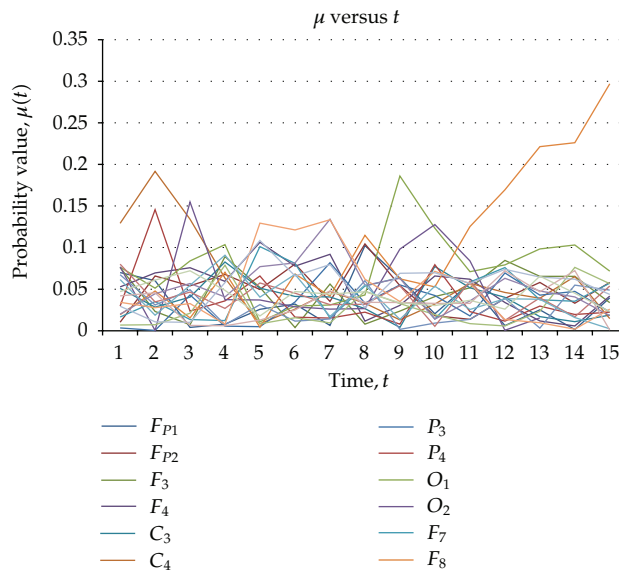


Figure 6: Plot of measure values over time for a 15-second seizure observed in Patient B.

Video footage taken during the seizure confirms that the patient experienced body spasms during ictal.

On the other hand, patient C (Figure 7), whose seizure lasts 25 seconds, exhibits a very focused fluctuation in potential difference, namely at electrodes F_{P1} and O_1 . Both these electrodes are at exact opposite ends of the left hemisphere of the brain, one being in the anterior region (F_{P1}), and the other at the posterior region (O_1). The graph also indicates that the readings at F_{P1} and O_1 are inversely proportional to each other, suggesting that the bulk

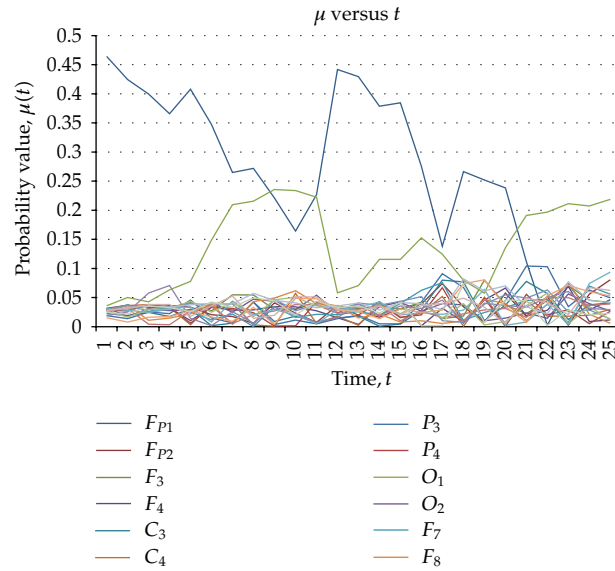


Figure 7: Plot of measure values over time for a 25-second seizure observed in Patient C.

of the electrical activity during Patient C’s seizure was moving back and forth between these two electrodes.

However, application of the Delia measure alone is insufficient to describe the progression of seizures, as it only reformats the data to fit in the $[0,1]$ interval. Based on the earlier assumption made in Section 5, more data regarding the pattern of EEG signals during a seizure may lie in higher dimensions. For this purpose, a mapping is developed to transfer the output of the Delia measure to a manifold.

7. Mapping Measure Data to a Manifold

This section covers the construction of a mapping from the set of Delia measure values to a high-dimensional manifold. To begin with, the set of selected output generated by applying the Delia measure is formalized as the *scaled potential set*.

Definition 7.1 (scaled potential set). The scaled potential set is the set of values generated by applying the Delia measure μ on singleton subsets of an electrode potential set, and is given by

$$V_t^\mu = \{\mu(A) \mid A \in P(V_t), \quad n(A) = 1\}, \tag{7.1}$$

Only the singleton subsets of the electrode potential sets are considered to form the scaled potential set. This is to ensure that each measure value in the set corresponds to only one potential difference, detected at a single electrode during the seizure. Since $\mu \in \mathbb{R}$ with $0 < \mu < 1$ and $\sum_{\mu \in V_t^\mu} \mu = 1$, each scaled potential set represents the discrete probability distribution of EEG signals observed at all electrodes $e \in E$ during any given time frame t during the seizure. Due to the nature of the data, and the intention of utilizing the vMF

distribution, the manifold required is a unit hypersphere. Transferring the contents of the V_t^μ to such a manifold is accomplished using Lemma 7.2.

Lemma 7.2 (spherical compatibility of probability values). *A discrete probability distribution with n outcomes can be represented as a point on a unit hypersphere.*

Proof. Consider a discrete probability distribution X with n outcomes, and let $\mu(x_i)$ denote the probability of each event $x \in X$ with respect to the measure μ . Then $X_\mu = \{\mu(x_1), \mu(x_2), \dots, \mu(x_n)\}$, and it follows that $0 < \mu(x_i) < 1$ for each $\mu(x_i)$, with $\sum_{x \in X} \mu(x_i) = 1$. By letting $\rho_i = \sqrt{\mu(x_i)}$ for each $x \in X$,

$$\begin{aligned} 1^2 = 1 &= \sum_{x \in X} \mu(x_i) \\ &= \sum_{x \in X} \rho_i^2, \end{aligned} \tag{7.2}$$

which is the general form for a unit hypersphere. \square

Bahlmann noted in 2006 that any probability distribution can be “wrapped” around the circumference of a circle with unit radius [53]. However, this approach was not utilized as it sacrifices information regarding the electrode of origin for each measure value. The following theorem is a direct result of Lemma 7.2.

Theorem 7.3 (EEG Signals as points on a hypersphere). *The EEG signals detected during a seizure can be viewed as points on the surface of a unit hypersphere.*

Proof. Given an epileptic seizure of length n seconds, n discrete electrode potential sets are constructed, each one representing the EEG potential differences detected at all connected electrodes at 1 s intervals. Using Definitions 5.8 and 7.1, n scaled potential sets are formed, namely, $V_1^\mu, V_2^\mu, \dots, V_n^\mu$. Suppose there are k electrodes in use. By Lemma 7.2, the positive square root of elements of each scaled potential set V_t^μ can be viewed as points on the surface of a k -dimensional unit hypersphere. Thus, by forming n scaled potential sets, the EEG signals detected at k electrodes during an epileptic seizure can be ported to points on a unit hypersphere of dimension k . \square

Definition 7.4 below formally defines the mapping from the scaled potential set to a unit hypersphere, whilst Definition 7.5 specifies the subset of the hypersphere that contains EEG recordings.

Definition 7.4 (EEG hypersphere map). The EEG hypersphere map, Θ , maps elements in a scaled potential set to the surface of a k -dimensional hypersphere and is given as

$$\Theta : \bigcup_{t=1}^n V_t^\mu \longrightarrow S_1^{k-1}, \tag{7.3}$$

where

$$\Theta(V_t^\mu) = (\sqrt{\mu_{e_1}}, \sqrt{\mu_{e_2}}, \dots, \sqrt{\mu_{e_k}}), \tag{7.4}$$

$\mu_{e_i} \in V_t^\mu$ refers to the Delia measure value corresponding to the potential difference detected at electrode e_i at time t .

The EEG hypersphere map, used in conjunction with the Delia measure, allows for the EEG signals of epileptic seizures to be viewed as points on the surface of a unit hypersphere. Using a spherical distribution such as the von Mises-Fisher distribution, further modelling of seizures can be carried out. However, the vMF modelling of seizures is not included in this paper, as the process involves estimating the concentration parameter κ , which is notoriously lengthy.

Definition 7.5 (the observed signal set). The observed signal set, O is the finite subset $\Theta(V_t^\mu) \subset S_1^{k-1}$.

With Definition 7.5, the following theorem takes form.

Theorem 7.6 (topology of EEG signals). *The observed signal set, O , is a topological space.*

Proof. Let (\mathbb{R}^k, Γ) be the standard k -dimensional Euclidean space with standard Euclidean topology Γ . Each $\tau \in \Gamma$ is given in the form $\tau_x = \{y \in \mathbb{R}^n \mid d(x, y) < \epsilon\}$, where d is the standard Euclidean metric, and $\epsilon > 0$. Define the topology for O to be Γ_O , where each $\psi \in \Gamma_O$ is in the form $\psi = \tau \cap O$. Then,

- (1) $\emptyset \in \Gamma_O$ since $\emptyset = \emptyset \cap O$ for $\emptyset \in \Gamma$,
- (2) $O \in \Gamma_O$ since $O = \mathbb{R}^k \cap O$ for $\mathbb{R}^k \in \Gamma$,
- (3) $\bigcup \psi \in \Gamma_O$ since

$$\begin{aligned} \bigcup \psi &= (\tau_1 \cap O) \cup (\tau_2 \cap O) \cup \dots \\ &= \left(\bigcup_i \tau_i \right) \cap O \\ &= \tau \cap O \quad \text{since } \tau = \bigcup_i \tau_i \in \Gamma, \end{aligned} \tag{7.5}$$

- (4) $\bigcap_{i=1}^k \psi_i \in \Gamma_O$ since

$$\begin{aligned} \bigcap_{i=1}^k \psi_i &= (\tau_1 \cap O) \cap (\tau_2 \cap O) \cap \dots \\ &= \left(\bigcap_{i=1}^k \tau_i \right) \cap O \\ &= \tau \cap O \quad \text{since } \tau = \bigcap_{i=1}^k \tau_i \in \Gamma. \end{aligned} \tag{7.6}$$

Thus (O, Γ_O) is a topological subspace, and hence a topological space. \square

The above proof that the seizure signals on the manifold constitutes a topological space verifies Ahmad's claim that a topological space can be constructed to house EEG signals of epileptic seizures [33].

8. Conclusion and Discussion

In this paper, measure theory was utilized to design the Delia measure, a discrete probability measure that reformats EEG data without altering its geometric structure. An analysis of EEG data from three patients experiencing epileptic seizures was made using the measure, with the resulting graph confirming the presence of symptoms such as behavioral changes and body spasms during recording. A mapping called the EEG hypersphere map then is devised to transport the measure data onto the surface of a unit hypersphere, thus allowing seizures to be viewed as a geometric structure. The authors suggest that further statistical analysis of seizures be carried out using the von Mises-Fisher distribution, justification for which is given in Section 5. The subset of seizure signals on the manifold is shown to be a topological space, verifying Ahmad's approach to use topological modelling.

Acknowledgments

The authors would like to thank the Ministry of Science, Technology and Innovation for funding this research under the Fundamental Research Grant Scheme (Vot. no. 78315) and the National Science Fellowship (NSF) Grant.

References

- [1] WHO, Epilepsy factsheet, 2009.
- [2] H. Gastaut, "Clinical and electroencephalographical classification of epileptic seizures," *Epilepsia*, vol. 11, no. 1, pp. 102–112, 1970.
- [3] T. Ahmad, R. A. Fairuz, F. Zakaria, and H. Isa, "Selection of a subset of EEG channels of epileptic patient during seizure using PCA," in *Proceedings of the 7th WSEAS International Conference on Signal Processing, Robotics and Automation*, pp. 270–273, World Scientific and Engineering Academy and Society (WSEAS), Stevens Point, Wis, USA, 2008.
- [4] F. Zakaria, *Dynamic profiling Of EEG data during seizure using fuzzy information space [Ph.D. thesis]*, Universiti Teknologi Malaysia, 2008.
- [5] E. Niedermeyer and F. H. L. Silva, *Electroencephalography: Basic Principles, Clinical Applications, and Related Fields*, M—Medicine Series, Lippincott Williams & Wilkins, 2005.
- [6] A. Babloyantz and A. Destexhe, "Low-dimensional chaos in an instance of epilepsy," *Proceedings of the National Academy of Sciences*, vol. 83, no. 10, pp. 3513–3517, 1986.
- [7] C. J. Stam, "Nonlinear dynamical analysis of EEG and MEG: review of an emerging field," *Clinical Neurophysiology*, vol. 116, no. 10, pp. 2266–2301, 2005.
- [8] L. D. Iasemidis, S. J. Chris, H. P. Zaveri, and W. J. Williams, "Phase space topography and the lyapunov exponent of electrocorticograms in partial seizures," *Brain Topography*, vol. 2, no. 3, pp. 187–201, 1990.
- [9] G. W. Frank, T. Lookman, M. A. H. Nerenberg, C. Essex, J. Lemieux, and W. Blume, "Chaotic time series analyses of epileptic seizures," *Physica D*, vol. 46, no. 3, pp. 427–438, 1990.
- [10] J. Theiler, "On the evidence for low-dimensional chaos in an epileptic electroencephalogram," *Physics Letters A*, vol. 196, no. 5-6, pp. 335–341, 1995.
- [11] N. Schiff, J. Victor, A. Canel, and D. Labar, "Characteristic nonlinearities of the 3/s ictal electroencephalogram identified by nonlinear autoregressive analysis," *Biological Cybernetics*, vol. 72, no. 6, pp. 519–526, 1995.

- [12] R. Friedrich and C. Uhl, "Spatio-temporal analysis of human electroen-cephalograms: petit-mal epilepsy," *Physica D*, vol. 98, no. 1, pp. 171–182, 1996.
- [13] J. L. Hernandez, P. A. Valds, and P. Vila, "EEG spike and wave modelled by a stochastic limit cycle," *NeuroReport*, vol. 7, no. 13, pp. 2246–2250, 1996.
- [14] M. Le van Quyen, J. Martinerie, C. Adam, and F. J. Varela, "Unstable periodic orbits in human epileptic activity," *Physical Review E*, vol. 56, no. 3, pp. 3401–3411, 1997.
- [15] M. Feucht, U. Miller, H. Witte et al., "Nonlinear dynamics of 3 hz spike- and-wave discharges recorded during typical absence seizures in children," *Cerebral Cortex*, vol. 8, no. 6, pp. 524–533, 1998.
- [16] T. E. Peters, N. C. Bhavaraju, M. G. Frei, and I. Osorio, "Network system for automated seizure detection and contingent delivery of therapy," *Journal of Clinical Neurophysiology*, vol. 18, no. 6, pp. 545–549, 2001.
- [17] C. E. Elger and K. Lehnertz, "Seizure prediction by non-linear time series analysis of brain electrical activity," *European Journal of Neuroscience*, vol. 10, no. 2, pp. 786–789, 1998.
- [18] J. Martinerie, C. Adam, M. Le van Quyen et al., "Epileptic seizures can be anticipated by non-linear analysis," *Nature Medicine*, vol. 4, pp. 1173–1176, 1998.
- [19] H. R. Moser, B. Weber, H. G. Wieser, and P. F. Meier, "Electroencephalograms in epilepsy: analysis and seizure prediction within the framework of lyapunov theory," *Physica D*, vol. 130, no. 3-4, pp. 291–305, 1999.
- [20] Y. C. Lai, M. A. F. Harrison, M. G. Frei, and I. Osorio, "Inability of lyapunov exponents to predict epileptic seizures," *Physical Review Letters*, vol. 91, no. 6, Article ID 068102, 4 pages, 2003.
- [21] I. Osorio, M. A. Harrison, Y. C. Lai, and M. G. Frei, "Observations on the application of the correlation dimension and correlation integral to the prediction of seizures," *Journal of Clinical Neurophysiology*, vol. 18, no. 3, pp. 269–274, 2001.
- [22] M. A. F. Harrison, I. Osorio, M. G. Frei, S. Asuri, and Y. C. Lai, "Correlation dimension and integral do not predict epileptic seizures," *Chaos*, vol. 15, no. 3, Article ID 33106, 2005.
- [23] S. Kalitzin, J. Parra, D. N. Velis, and F. H. Lopes da Silva, "Enhancement of phase clustering in the EEG/MEG gamma frequency band anticipates transitions to paroxysmal epileptiform activity in epileptic patients with known visual sensitivity," *IEEE Transactions on Biomedical Engineering*, vol. 49, no. 11, pp. 1279–1286, 2002.
- [24] W. van Drongelen, S. Nayak, D. M. Frim et al., "Seizure anticipation in pediatric epilepsy: use of kolmogorov entropy," *Pediatric Neurology*, vol. 29, no. 3, pp. 207–213, 2003.
- [25] F. Mormann, R. G. Andrzejak, C. E. Elger, and K. Lehnertz, "Seizure prediction: the long and winding road," *Brain*, vol. 130, no. 2, pp. 314–333, 2007.
- [26] P. McSharry, T. He, L. Smith, and L. Tarassenko, "Linear and non-linear methods for automatic seizure detection in scalp electro-encephalogram recordings," *Medical and Biological Engineering and Computing*, vol. 40, no. 4, pp. 447–461, 2002.
- [27] D. Kugiumtzis and P. G. Larsson, "Prediction of epileptic seizures with linear and nonlinear analysis of EEG," in *Chaos in Brain?: Proceedings of the Workshop*, K. Lehnertz and C. E. Elger, Eds., pp. 329–332, World Scientific, 1999.
- [28] K. K. Jerger, T. I. Netoff, J. T. Francis et al., "Early seizure detection," *Journal of Clinical Neurophysiology*, vol. 18, pp. 259–268, 2001.
- [29] S. Baillet and L. Garnero, "A bayesian approach to introducing anatomo-functional priors in the EEG/MEG inverse problem," *IEEE Transactions on Biomedical Engineering*, vol. 44, no. 5, pp. 374–385, 1997.
- [30] J. R. Stevens, "Electroencephalographic studies of conditional cerebral response in epileptic subjects," *Electroencephalography and Clinical Neurophysiology*, vol. 12, no. 2, pp. 431–444, 1960.
- [31] O. Faust, R. U. Acharya, A. R. Allen, and C. M. Lin, "Analysis of eeg signals during epileptic and alcoholic states using ar modeling techniques," *Ingénierie et Recherche Biomédicale*, vol. 29, no. 1, pp. 44–52, 2008.
- [32] N. Sivasankari and K. Thanushkodi, "Automated epileptic seizure detection in EEG signals using fast ICA and neural networks," *International Journal of Soft Computing Applications*, vol. 1, no. 2, 2009.
- [33] T. Ahmad, R. S. Ahmad, F. Zakaria, and L. L. Yun, "Development of detection model for neuro-magnetic fields," in *Proceedings of the BIOMED 2000*, pp. 119–121, University of Malaya, September 2000.
- [34] T. Ahmad, R. S. Ahmad, W. E. Z. W. Abdul Rahman, L. L. Yun, and F. Zakaria, "Fuzzy topographic topological mapping for localisation simulated multiple current sources of MEG," *Journal of Interdisciplinary Mathematics*, vol. 11, pp. 381–393, 2008.

- [35] A. Idris, T. Ahmad, and N. Maan, "A novel technique for visualization electrical activities in the brain during epileptic seizure," in *Proceedings of the International Conference on Applied Mathematics and Informatics*, pp. 94–99, 2010.
- [36] J. M. Franks, *Terse Introduction to Lebesgue Integration*, Student mathematical library, American Mathematical Society, Providence, RI, USA, 2009.
- [37] S. K. Berberian, *Measure and Integration*, AMS Chelsea Publishing, Providence, RI, USA, 2011.
- [38] G. G. Roussas, *An Introduction to Measure-Theoretic Probability*, Elsevier / Academic Press, Amsterdam, The Netherlands, 2005.
- [39] W. J. Ewens and G. R. Grant, *Statistical Methods in Bioinformatics: An Introduction*, vol. 10 of *Statistics for Biology and Health*, Springer, New York, NY, USA, 2005.
- [40] M. J. Hassett and D. Stewart, *Probability for Risk Management*, ACTEX academic series, ACTEX Publications, 2006.
- [41] R. R. Wilcox, *Introduction to Robust Estimation and Hypothesis Testing*, Statistical Modeling and Decision Science, Elsevier Science & Technology, 1997.
- [42] A. Banerjee, I. S. Dhillon, J. Ghosh, and S. Sra, "Clustering on the unit hypersphere using von Mises-Fisher distributions," *Journal of Machine Learning Research*, vol. 6, pp. 1345–1382, 2005.
- [43] E. Zakon, B. Lucier, and T. Zakon, *Mathematical Analysis*, The Zakon Series on Mathematical Analysis, The Trillia Group, 2004.
- [44] A. Dold, *Lectures on Algebraic Topology*, Classics in Mathematics, Springer, Berlin, Germany, 1995.
- [45] S. I. Amari, H. Nagaoka, and D. Harada, *Methods of Information Geometry*, Translations of Mathematical Monographs, American Mathematical Society, Providence, RI, USA, 2007.
- [46] J. M. Lee, *Introduction to Topological Manifolds*, vol. 202 of *Graduate Texts in Mathematics*, Springer, New York, NY, USA, 2011.
- [47] S. Lipschutz, *Schaum's Outline of General Topology*, McGraw-Hill, 1988, Série Schaum.
- [48] Y. Eidelman, V. D. Milman, and A. Tsolomitis, *Functional Analysis: An Introduction*, Graduate Studies in Mathematics, American Mathematical Society, Providence, RI, USA, 2004.
- [49] J. Malmivuo and R. Plonsey, *Bioelectromagnetism: Principles and Applications of Bioelectric and Biomagnetic Fields*, Oxford University Press, 1995.
- [50] J. W. B. Douglas, "A neuropsychiatric study in childhood by Michael Rutter, Philip Graham and William Yule, clinics in developmental medicine, volume 35/36. (pp. 272; illustrated; 375.) heinemann medical books: London. 1970," *Psychological Medicine*, vol. 1, no. 5, pp. 437–439, 1971.
- [51] S. McDermott, S. Mani, and S. Krishnawami, "A population-based analysis of specific behavior problems associated with childhood seizures," *Journal of Epilepsy*, vol. 8, no. 2, pp. 110–118, 1995.
- [52] L. M. Surhone, M. T. Tennoe, and S. F. Henssonow, *Premotor Cortex*, VDM Verlag Dr. Mueller AG & Co. Kg, 2010.
- [53] C. Bahlmann, "Directional features in online handwriting recognition," *Pattern Recognition*, vol. 39, pp. 115–125, 2006.



Hindawi

Submit your manuscripts at
<http://www.hindawi.com>

